CRYSTAL GROWTH & DESIGN

Article

pubs.acs.org/crystal

Crystallization of Microparticulate Pure Polymorphs of Active Pharmaceutical Ingredients Using CO_2-Expanded Solvents

Published as part of a virtual special issue of selected papers presented at the 9th International Workshop on the Crystal Growth of Organic Materials (CGOM9)

Santiago Sala,[†,‡] Alba Córdoba,[†,‡] Evelyn Moreno-Calvo,[‡,†] Elisa Elizondo,[‡,†] Maria Muntó,[‡,†] Paula Elena Rojas,[‡,†] Maria Àngels Larrayoz,[§] Nora Ventosa,*[,‡,†] and Jaume Veciana*[,‡,†]

[†]CIBER de Bioingeniería, Biomateriales y Nanomedicina (CIBER-BBN)

[‡]Department of Molecular Nanoscience and Organic Materials. Institut of Materials Science of Barcelona (ICMAB-CSIC), Campus de la UAB, 08193, Bellaterra, Spain

[§]Universitat Politècnica de Catalunya, Chemical Engineering Department, ETSEIB, Avda, Diagonal 647, 08028 Barcelona, Spain

ABSTRACT: The feasibility of the Depressurization of an Expanded Liquid Organic Solution (DELOS) method to process different active pharmaceutical ingredients (APIs) as finely divided powders with narrow particle size distribution, high crystallinity degree, high polymorphic purity, and free from residual solvent has been demonstrated. Cholesterol, acetylsalicylic acid (aspirin), naproxen, acetaminophen, and ibuprofen were chosen as model drugs. It has been demonstrated that the supersaturation ratio attained during crystallization from CO_2-expanded solvents can be modulated through appropriate variations of process parameters — CO_2 content and concentration of the initial solution. In view of the potential application that compressed fluids-based technologies have in the pharmaceutical industry, a preliminary scalability study of the process in compliance with the constraints imposed by the Good Manufacturing Practices (GMP) specifications is presented herein.

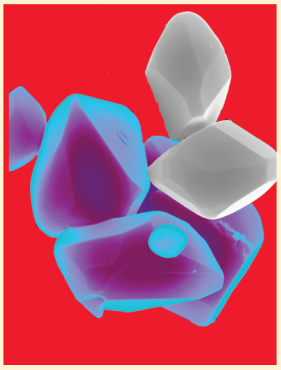

1. INTRODUCTION

The 21st century challenge in the pharmaceutical industry does not exclusively focus on the development of new therapeutic molecules but is also concerned with the search for better delivery routes and combined formulations to increase bioavailability of already developed drugs. Development of new drugs is expensive, risky, and slow, taking up to 15 years to obtain full accreditation, so pharmaceutical companies are keen to investigate new formulations that can deliver or target existing drugs more effectively. Among others, one strategy consists of the preparation of active ingredients as micro- and nanoparticulate solids, since the therapeutic activity of pharmaceutical entities is related to the chemical structure but also to physical factors such as crystallinity, polymorphism, and particle size. Effective administration of the majority of new developed pharmaceutical drugs is related to the control over their pharmacokinetic properties through physical modification.[1] Fine particles with a narrow particle size distribution, which have a high surface area, generally increase the bioavailability and dissolution rate of pharmaceuticals.[2] For example, drugs administered orally are limited by its dissolution rate in the gastrointestinal tract. In addition, prescribed doses can be reduced by improving the drug dissolution rate in the biological environment.[3] Therapeutic compounds in the form of micropowders offer convenient and controllable delivery by subcutaneous, intramuscular, topical, and intestinal modes. Controlled particle characteristics also create opportunities for alternative delivery systems to be explored, such as powder injection (a needle-free technique for the transdermal delivery of micronized drugs).[4] Particle size is one of the critical factors for the determination of appropriate administration routes. The ideal micrometer-sized pharmaceutical should retain the original crystallinity, polymorphism, and chemical activity of the raw material and should be in the form of free-flowing, nonaggregated, monodispersed, and polymorphically pure powder.

Standard procedures for generating particulate solids are usually multistep processes consisting of a precipitation/crystallization followed by additional downstream steps for particle size reduction and homogenization. Even though these methodologies are still the most used, they are not always adequately responsive to market and clinical demands because of undesired product transformations (i.e., polymorphic transitions), inapplicability to thermolabile or waxy materials, low batch-to-batch reproducibility, and complex scale-up. Besides, crystallization/precipitation from liquid solvents is limited by the low control over particle size distribution and also by the difficulty of complying with residual solvent acceptable limits imposed by regulatory agencies, for example, ICH Guidelines or pharmacopoeias.[5] Many industrial solvents

Received: March 21, 2011
Revised: January 2, 2012
Published: February 13, 2012

dx.doi.org/10.1021/cg200356x | *Cryst. Growth Des.* 2012, 12, 1717–1726

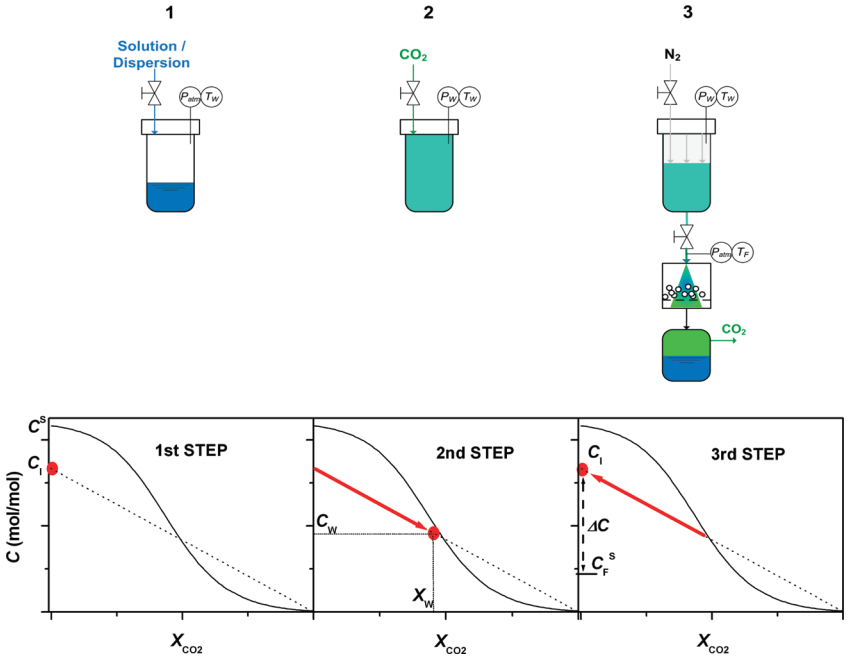

Figure 1. Top: DELOS steps. Bottom: Example of the evolution of the solute concentration at each of the three steps of the process (red points) in relation to the solubility curve of the solute in the CO_2-expanded solvent (black solid line), at a working pressure P_W and working temperature T_W.

are not only hazardous (toxic, flammable, etc.), but their full recovery and recycling are often not easy.

In recent years, several particle formation techniques based upon the utilization of compressed fluids (CF) as crystallization media have been developed.[6−8] Most of these technologies have in common the use of CO_2 as CF since it is nontoxic, nonflammable, cheap, and easily recyclable. Among these, in the past decade we have reported the Depressurization of an Expanded Liquid Organic Solution (DELOS) process, which involves the use of a CF for the one-step production of micrometer-sized and sub-micrometer-sized crystalline particles of high polymorphic purity and morphological homogeneity.[9−11] The driving force of this crystallization process is the fast, large, and extremely homogeneous temperature decrease experienced by a solution of the compound to crystallize in an organic solvent expanded with a CF, when it is depressurized from a given working pressure to atmospheric pressure. This method presents a new and interesting route for pharmaceutical particle formation which avoids most drawbacks of traditional methods. The methodology is shown in Figure 1 and has been extensively described elsewhere.[9−11]

The first step of this process consists of the dissolution of the drug in a conventional organic solvent, at atmospheric pressure and working temperature (T_W), to form a solution with an initial concentration C_I. Second, the initial solution is pressurized up to the working pressure (P_W) by the addition of a given amount of CO_2, expressed by the CO_2 molar fraction of the mixture "organic solvent/CO_2" (X_W). In this second step, the solute concentration (C_W) should remain below the saturation limit in the CO_2-expanded mixture, that is, the solute is soluble in the CO_2-expanded mixture showing a single liquid phase. In the third step, the solution is depressurized from the working pressure P_W to atmospheric pressure, through a nonreturn simple valve. During this depressurization step, the CO_2 evaporates very rapidly from the solution producing a large, fast, and extremely homogeneous decrease of the solution temperature down to a final temperature, T_F. Differently from conventional cooling crystallization processes, it can be assumed that in this case, T_F is reached before primary nucleation takes place and therefore, as schematized in Figure 1, the initial solute concentration is re-established ($C_F = C_I$) during this third step. The consequence of this abrupt temperature decrease ΔT ($\Delta T = T_F - T_W$) is a fast, pronounced, and very homogeneous increase of the supersaturation all over the solution — C_F becomes higher than the solute solubility in the conventional solvent at the final temperature, C_F^S — causing the precipitation of finely divided crystalline powders with narrow particle size distribution. Under the conditions of the DELOS crystallization, it could be considered that the difference between C_I and C_F^S, ΔC ($\Delta C = C_I - C_F^S$) is the maximum supersaturation achieved and the supersaturation ratio can be calculated as $S = C_I / C_F^S$. Thus, the higher ΔC, the higher the maximum supersaturation attained, and more favored will be nucleation over crystal growth, provoking the crystallization of small particles.[12]

In the present work, we demonstrate the feasibility of producing micrometer-sized particles using this process, with narrow particle size distribution and high polymorphic purity, of five different pharmaceutical active ingredients. In the first part, the relationship between process parameters carbon dioxide content X_W and initial concentration C_I, with the crystallization conditions achieved during the depressurization of the CO_2-expanded solution (final temperature T_F and solubility at final temperature C_F^S), is described. In the second part, the crystallization outcome (yield and particle size) is discussed in relation to the supersaturation ratio S attained in the third step due to the abrupt and homogeneous temperature decrease. The specific weight of process parameters C_I and X_W on the supersaturation ratio and therefore on particle characteristics has been studied, and a procedure to predict the parameter importance, related to drug solubility behavior, is presented. Aspirin (ASP) and acetaminophen (ACPH), as analgesic and antipyretic compounds, ibuprofen (IBU) and naproxen (NAP), as nonsteroidal anti-inflammatory agents, and

dx.doi.org/10.1021/cg200356x | Cryst. Growth Des. 2012, 12, 1717−1726

cholesterol (COL), as a steroid model compound, are the drugs chosen to carry out this study (Scheme 1). These drugs show distinct lipophilicity degrees and large differences in water solubility, being therefore representative of different types of pharmaceutical active compounds. Particle size distribution, morphology, crystallinity, and crystalline nature of the powders obtained have been characterized. In relation to the industrial viability of the process, a desirable manufacturing method for the processing of APIs should be easily scalable, economically viable, and easily compliant with the restrictions of Good Manufacturing Practices (GMPs). Because of this, the process studied has emerged as a promising green, scalable, and industrially viable methodology, as the results of a very recent study show,[13] which are summarized in the final section.

Scheme 1. Molecular Formula of Selected Drugs[a]

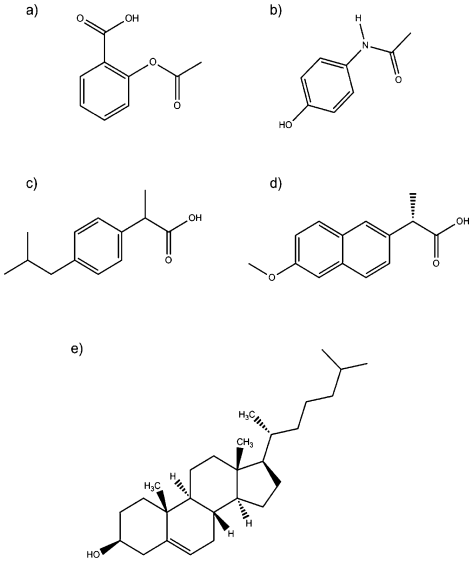

[a](a) Aspirin (ASP), (b) acetaminophen (ACPH), (c) ibuprofen (IBU), (d) naproxen (NAP), and (e) cholesterol (COL).

2. MATERIALS AND METHODS

2.1. Materials and Solvents. Aspirin (99.5%), acetaminophen (99%), cholesterol (99%), ibuprofen (99%), and naproxen (98%) were purchased from SIGMA-Aldrich (Steinheim, Germany). Concerning solvents, acetone (99.5%) was bought from QUIMIVITA (Barcelona, Spain), and ethanol (99.5%) from PANREAC (Barcelona, Spain). CO_2 (purity 99.995%) was supplied by Carburos Metálicos S.A. (Barcelona, Spain). All chemicals were employed without further purification.

2.2. Experimental Details of Crystallizations. Crystallization experiments were performed according to the usual three steps represented in Figure 1. Acetone or ethanol was employed as conventional organic solvents. Experimental apparatus and procedures used to perform crystallization experiments are described in detail in previous works.[9−11] A known volume of a solution of the API in an organic solvent, of known initial concentration C_I was loaded in a lab-scale high-pressure vessel (300 mL). During all experiments the working temperature T_W was kept constant. The initial solution was then pressurized up to the desired working pressure P_W by addition of a given amount of CO_2, X_W. After leaving the system under the same conditions for 30−60 min to achieve complete homogenization and thermal equilibration, the solution was depressurized over a nonreturn valve from P_W to atmospheric pressure. When the solution depressurization started, the temperature, registered after the depressurization valve, decreased suddenly until reaching a constant value. This final temperature value was taken as T_F and the temperature decrease was calculated as follows: $\Delta T = T_F - T_W$. The precipitated particles were recovered on a filter (pore size 200 nm). After filtration the recovered particles were dried with a CO_2 flow at 40 bar for 30 min.

2.3. Drug Particle Characterizations. Particle size distributions were measured with a laser diffraction particle size analyzer (Beckman Coulter model LS13320). Water with 0.1% (v/v) of polyoxyethylene (20) sorbitan monooleate (Tween 80) was employed as a dispersing medium in cholesterol, naproxen, and ibuprofen measurements, whereas a high-boiling point petroleum fraction was used in aspirin and acetaminophen particle size determinations. Particles morphology was observed using a HITACHI model S-570 scanning electron microscope (SEM). Powder X-ray diffraction analyses were performed using a RIGAKU DS5000 diffractometer to ascertain if changes in crystallinity and polymorphism occurred after drug processing. For each sample, powder X-ray diffraction patterns were collected during 1 h between 2θ angles of 3 and 40. Thermogravimetric analyses (TGA) were performed to evaluate residual solvent amounts in the processed samples. These analysis were recorded with a STA 449-F1 Jupiter (NETZSCH), using the *NETZSCH Proteus* software. Samples of

Table 1. Operating Conditions, Cooling, and Supersaturation Ratios Achieved in Crystallization Experiments of the Selected Model Drugs from CO_2-Expanded Solvents

exp[a]	solvent	P_W (MPa)	T_W (K)	C_I[b] (mol/mol)	X_W[c]	T_F[d] (K)	ΔT[e] (K)	C_F^S[f] (mol/mol)	ΔC[g] (mol/mol)	S[h]
ASP1	acetone	7	295	7.0×10^{-2}	0.40	268	−27	5.6×10^{-2}	0.014	1.3
ASP2	acetone	7	295	7.0×10^{-2}	0.47	262	−33	4.8×10^{-2}	0.022	1.5
ASP3	acetone	7	295	5.2×10^{-2}	0.55	247	−48	2.8×10^{-2}	0.024	1.9
ASP4	acetone	7	295	3.5×10^{-2}	0.55	247	−48	2.8×10^{-2}	0.007	1.3
ASP5	ethanol	7	298	8.1×10^{-2}	0.55	234	−64	4.8×10^{-3}	0.076	17
COL1	acetone	10	308	5.1×10^{-3}	0.50	258	−50	6×10^{-4}	0.0045	9
COL2	acetone	10	308	5.1×10^{-3}	0.64	248	−60	3×10^{-4}	0.0048	17
COL3	acetone	10	308	3.8×10^{-3}	0.71	238	−70	3×10^{-4}	0.0035	13
COL4	acetone	10	308	2.6×10^{-3}	0.71	233	−75	3×10^{-4}	0.0023	9
NAP1	ethanol	10	298	8.8×10^{-3}	0.80	208	−90	2.3×10^{-3}	0.007	4
IBU1	acetone	10	298	1.7×10^{-1}	0.80	223	−75	1.8×10^{-2}	0.152	9
ACPH1	ethanol	10	315	6.6×10^{-2}	0.40	275	−40	3.4×10^{-2}	0.032	2

[a]ASP means aspirin; COL means cholesterol; NAP means naproxen; IBU means ibuprofen; ACPH means acetaminophen. [b]C_I is the concentration of solute in the initial organic solution. [c]CO_2 content, X_W = CO_2 molar fraction in the solvent mixture. [d]Temperature achieved at the depressurization step, when the crystallization takes place. [e]Temperature decrease, $\Delta T = T_F - T_W$. [f]C_F^S is the solubility of the compound in the organic solvent at T_F. These solubilities were measured gravimetrically. [g]Absolute supersaturation, $\Delta C = C_I - C_F^S$. [h]Supersaturation ratio $S = C_I/C_F^S$.

dx.doi.org/10.1021/cg200356x | *Cryst. Growth Des.* 2012, 12, 1717−1726

approximately 15 mg were weighed into 100 μL aluminum pans and heated at 5 K min^{-1} from 298 to 380, 443, and 473 K for ibuprofen, aspirin, and naproxen, respectively, under nitrogen (60 mL/min).

3. RESULTS AND DISCUSSION

3.1. Crystallization Conditions of Aspirin, Cholesterol, Naproxen, Ibuprofen, and Acetaminophen. Table 1 summarizes the operating conditions of crystallization experiments of model drugs aspirin (ASP), cholesterol (COL), naproxen (NAP), ibuprofen (IBU), and acetaminophen (ACPH). For each experiment is shown the final temperature T_F achieved during the depressurization, when the crystallization occurs, and the solubility of each compound at T_F (C_F^S), which allows the calculation of the corresponding absolute supersaturation ΔC and the supersaturation ratio S achieved. Aspirin and cholesterol were processed at different values of initial concentration C_I and CO_2 molar fraction X_W. The effect of these parameters on the supersaturation generated and hence on particle size is discussed in section 3.2.

Appropriate operating conditions C_I and X_W were chosen according to solubility behavior of the different drugs in the corresponding "organic solvent/CO_2" mixtures, so that in the second step of the process the CO_2-expanded mixture presents a single liquid phase; see Figure 1. For achieving successful crystallizations, experiment conditions must ensure the preservation of the experiments in the liquid region of the system, along or close below the solubility curve. The solubility curve of aspirin in CO_2-expanded acetone,[14] and working conditions of experiments ASP2 and ASP3 are represented in Figure 2. As the Figure shows, crystallization experiments ASP2 and ASP3 are situated along the solubility curve. Solubility curves of aspirin in CO_2-expanded ethanol, and those of cholesterol, naproxen, ibuprofen and acetaminophen in the corresponding CO_2-expanded solvents are described in previous work.[15−18]

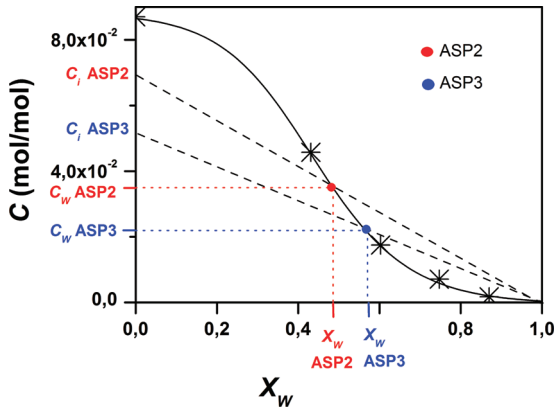

Figure 2. Solubility curve (continuous line) fitted through experimental solubility data (*) of aspirin (found in ref 9) in CO_2-expanded acetone, and working points of experiments ASP2 and ASP3 at P_W = 7 MPa and T_W = 295 K. Working lines (black dashed lines) depict the evolution of the solute concentration by addition of pure CO_2 in experiments ASP2 and ASP3.

As shown in Table 1, the higher the CO_2 content in the mixture (X_W), the higher the temperature decrease (ΔT) achieved. The explanation for this is the following. In the depressurization step, CO_2 evaporates and takes the heat required for its vaporization from the organic solution in which it was dissolved, causing an abrupt temperature decrease. Therefore, increasing the CO_2 amount in the mixture results in an increase of the heat required for the CO_2 phase change, and thereby a larger solution temperature decrease, ΔT, is observed.[9−11] In contrast with conventional cooling crystallizations, the temperature decrease in a DELOS process is ideally homogeneous, since the extension of the CO_2 evaporation is exactly the same throughout the solution, causing an extremely homogeneous increase of the supersaturation over all the solution. The large supersaturation, rapidly and homogeneously achieved, is the reason why micrometer-sized powders with low polydispersitivity are obtained. The table also shows for each experiment the corresponding API solubility in the organic solvent at the depressurization temperature (C_F^S). The high solubility variation from T_W to T_F generates a supersaturation of the solution and the crystallization of the drug particles.

Experiments ASP1-ASP2 and CHOL1-CHOL2 show that for given operating conditions, increasing X_W results in an increase of ΔT. In experiments ASP1-ASP2, an increase in X_W from 0.40 to 0.47 results in an increase in ΔT from −27 K to −33 K. Experiments COL1-COL2 show that increasing X_W from 0.50 to 0.64 results in an increase from −50 K to −60 K in ΔT. Since in these conditions the solubility decreases with a decrease of the depressurization temperature, the absolute supersaturation and the supersaturation ratio achieved in ASP2 (ΔC = 0.022 mol/mol; S = 1.5) and CHOL2 (ΔC = 0.0048 mol/mol; S = 17) are higher than in ASP1 (ΔC = 0.014 mol/mol; S = 1.3) and CHOL1 (ΔC = 0.0045 mol/mol; S = 9) respectively. In conclusion, increasing the CO_2 content results in an increase of the supersaturation attained in the crystallization experiments. The solubility variation with temperature depends on the compound and solvent nature. Aspirin solubility in acetone decreases linearly with temperature in the range from 250 to 300 K, while cholesterol solubility in ethanol shows an exponential behavior, and no significant solubility variation is observed below 275 K (see Figure 5).

On the other hand, experiments ASP3-ASP4 and CHOL3-CHOL4 were performed at different initial concentrations C_I, keeping constant the rest of the operating parameters. As experiments ASP3-ASP4 show, increasing the initial concentration from 3.5 × 10^{-2} mol/mol to 5.2 × 10^{-2} mol/mol provokes an increase of the supersaturation ratio S from 1.3 to 1.9. Regarding cholesterol crystallization experiments COL3-COL4, increasing C_I from 2.6 × 10^{-3} mol/mol to 3.8 × 10^{-3} mol/mol also results in an increase in S from 9 to 13. Therefore, increasing the initial concentration C_I provokes an increase of the supersaturation achieved in the crystallizations.

3.2. Crystallization Outcome. Powder Characterization and Effect of Process Parameters on Particle Size. In all experiments summarized in Table 1 finely divided powders with micrometric size and homogeneous and defined morphology were obtained. Figure 3 shows some representative SEM images of the particles produced by the crystallization experiments. Crystals of aspirin and cholesterol consist of finely shaped prisms with irregular edges and very well developed basal faces. Plate-like crystals of homogeneous morphology and with very developed basal faces are obtained from the crystallization of naproxen. Aspirin, cholesterol, and naproxen crystals have an especially low aspect ratio. Ibuprofen particles show plate-like crystals of irregular shape. Acetaminophen processed particles show well-faceted prismatic crystals.

The particulate samples of the model drugs produced by the process studied were highly crystalline and consisted of pure

dx.doi.org/10.1021/cg200356x | Cryst. Growth Des. 2012, 12, 1717−1726

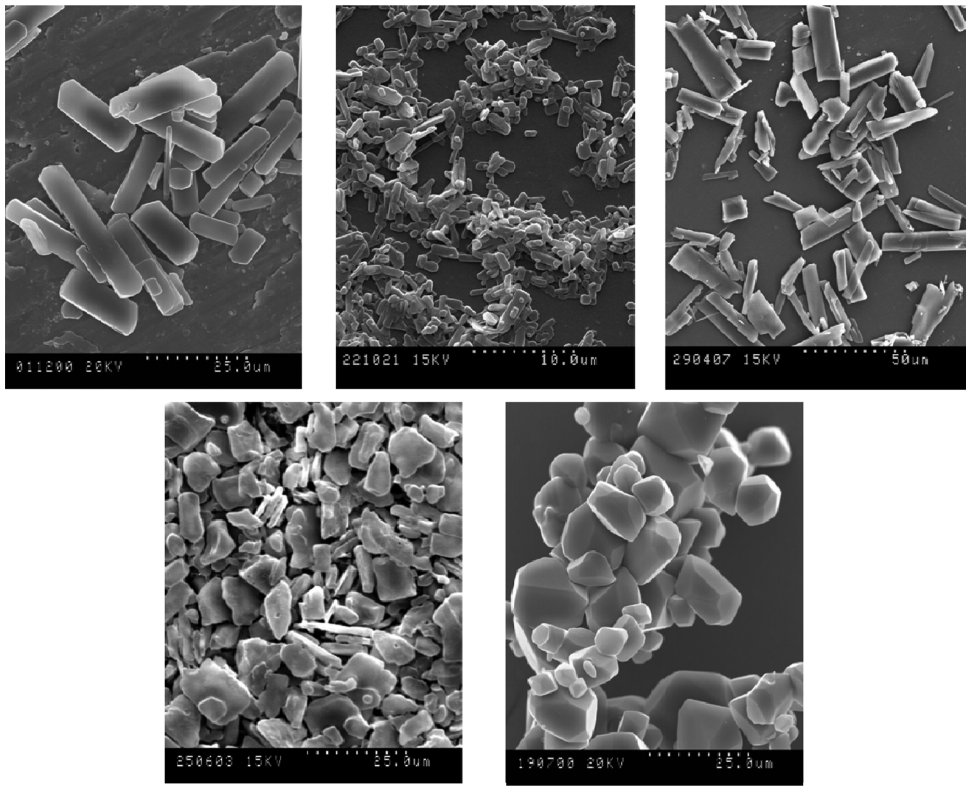

Figure 3. SEM images of DELOS processed drugs. Top images, from left to right: aspirin, experiment ASP3; cholesterol, experiment COL2, naproxen, experiment NAP1. Bottom images, from left to right: ibuprofen, experiment IBU1 and acetaminophen, experiment ACPH1.

polymorphic phases, as happened when processing stearic acid.[19] As can be seen in Figure 4, powder X-ray diffraction (PXRD) patterns of processed aspirin particles and raw aspirin particles correspond to the most usual polymorph of aspirin described so far, the PXRD pattern of which has been simulated from its crystalline structure.[20,21] Some differences in the relative peak intensities of raw aspirin are found probably due to the preferred orientation of microcrystals caused by the high particle size and plate-like morphology of the starting material. Processed cholesterol and raw cholesterol show the same PXRD pattern and correspond to the anhydrous and most stable polymorph of cholesterol at room temperature.[22] The PXRD pattern of this polymorph has been simulated from the single crystal structure. The same results concerning polymorphism were observed when comparing naproxen, acetaminophen, and ibuprofen processed by the method studied with their corresponding starting materials (also shown in Figure 4), after processing the crystal form is the same as that of the starting material. This form corresponds to the most stable polymorph of acetaminophen,[23] and the other to the only reported crystalline structures of naproxen[24] and ibuprofen.[25] Starting materials lead to PXRD patterns with some variations on peak relative intensities in relation to those obtained from the processed particles patterns probably due to preferred orientation. By TG analysis we have observed that the amount of residual solvent in all processed samples is below the standard ICH acceptable limits for class 3 solvents (5000 ppm).[5] TG analyses do not show mass lost during heating from room temperature to 373.15 K, so there is no need for further drying steps.

3.2.1. Effect of Operational Parameters on Drug Particle Size. Table 2 shows the crystallization yields and particle size distributions obtained, as well as the real supersaturation ratio S achieved in each crystallization experiment, which has been calculated from the initial concentration C_I and the drug solubility at the depressurization temperature C_F^S (shown in Table 1).

Different particle size distributions were obtained depending on the operating conditions. Crystallization of aspirin from CO_2-expanded acetone gave powder samples with a medium particle diameter between 14 and 31 μm, depending on the operating conditions. By processing cholesterol from the same solvent mixture, particle sizes between 0.5 and 2 μm were straightforwardly achieved. Volumetric particle size distributions show an important fraction (10%) of cholesterol particles included in the sub-micrometer range. The low uniformity index indicates a narrow particle size distribution. Naproxen processed particles have a medium particle size of 10 μm. Ibuprofen particles present a medium particle size of 8 μm, while acetaminophen particles have a medium diameter of 19 μm.

Crystallization experiments of aspirin (ASP) and cholesterol (COL), shown in Table 1, were carried out at different values of initial solute concentration (C_I) and CO_2 molar fraction (X_W) to gain a better insight into the effects of these operational parameters on the characteristics of the processed drugs, in terms of particle size.

Experiments ASP1-ASP2 and COL1-COL2 were performed over initial solutions of aspirin and cholesterol, respectively, varying the CO_2 content, X_W, while keeping constant the rest of process parameters. As shown in Table 2, under these conditions, aspirin medium particle size decreases from 31.4 to 23.4 μm when X_W is increased from 0.40 to 0.47, and cholesterol medium particle size decreases from 1.2 to 0.5 μm

dx.doi.org/10.1021/cg200356x | *Cryst. Growth Des.* 2012, 12, 1717–1726

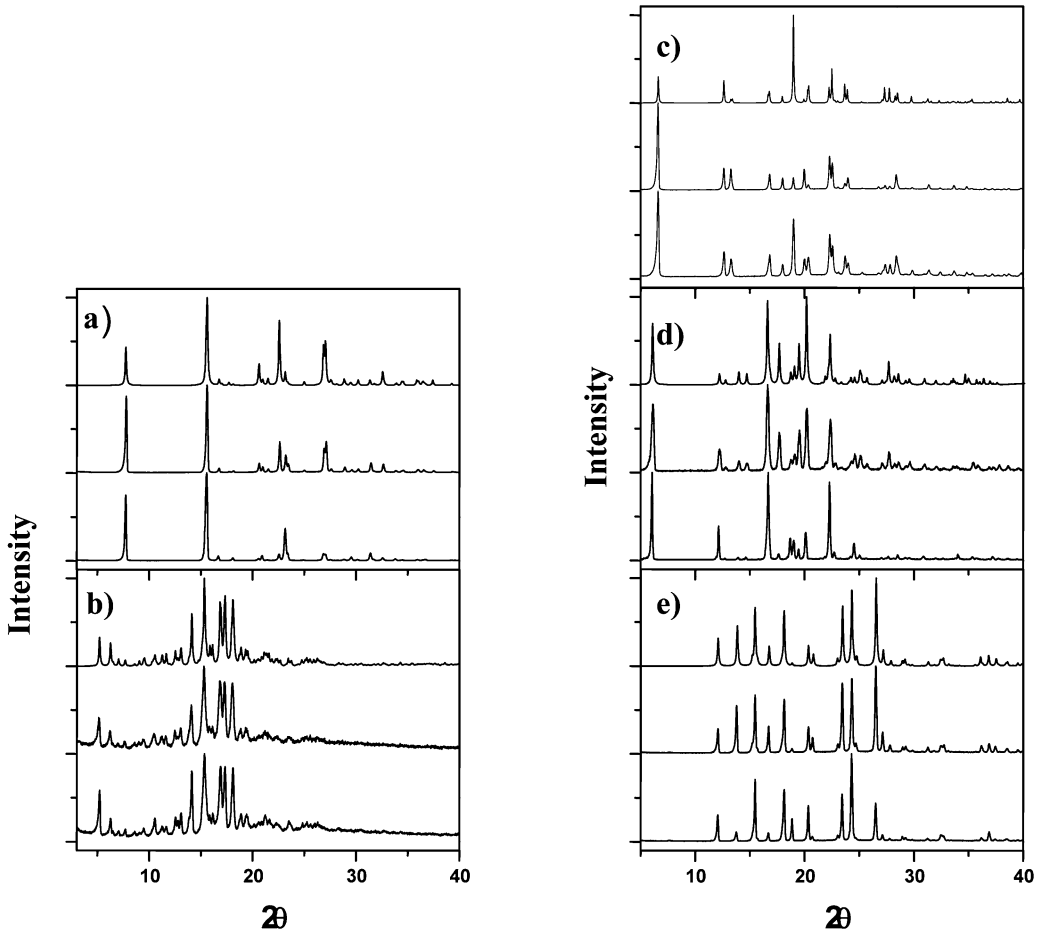

Figure 4. X-ray powder diffraction spectra of (a) aspirin; (b) cholesterol; (c) naproxen; (d) acetaminophen; and (e) ibuprofen. For each product the lower trace corresponds to the pattern of the starting material, the middle one to the processed particles, and the upper to the simulated diffractograms of the most common polymorph reported for aspirin, the most stable polymorph of cholesterol at room temperature, acetaminophen polymorph I and the unique reported ibuprofen crystalline structure.

Table 2. Supersaturation and Crystallization Outcome: Yield and Particle Size Distribution

								particle size[h] (μm)			
exp[a]	solvent	C_I [b](mol/mol)	X_W [c]	ΔT[d] (K)	ΔC[e] (mol/mol)	S[f]	yield[g] (%)	$d(0.1)$	$d(0.5)$	$d(0.9)$	UI[i]
ASP1	acetone	7.0×10^{-2}	0.40	−27	0.014	1.3	20	10.5	31.1	73.7	14
ASP2	acetone	7.0×10^{-2}	0.47	−33	0.022	1.5	30	8.1	23.4	59.2	14
ASP3	acetone	5.2×10^{-2}	0.55	−48	0.024	1.9	40	5.9	16.5	42.6	14
ASP4	acetone	3.5×10^{-2}	0.55	−48	0.007	1.3	10	4.3	30.5	58.0	7
ASP5	ethanol	8.1×10^{-2}	0.55	−64	0.076	17	80	3.9	13.7	27.3	14
COL1	acetone	5.1×10^{-3}	0.50	−50	0.0045	9	80	0.3	1.2	9.3	3
COL2	acetone	5.1×10^{-3}	0.64	−60	0.0048	17	85	0.2	0.5	4.5	4
COL3	acetone	3.8×10^{-3}	0.71	−70	0.0035	13	85	0.3	1.2	6.0	5
COL4	acetone	2.6×10^{-3}	0.71	−75	0.0023	9	75	0.5	2.1	10.0	5
NAP1	ethanol	8.8×10^{-3}	0.80	−90	0.007	4	50	6.0	10.0	35.0	17
IBU1	acetone	1.7×10^{-1}	0.80	−75	0.152	9	60	3.5	8.0	17.0	21
ACPH1	ethanol	6.6×10^{-2}	0.40	−40	0.032	2	10	3.5	18.6	34.5	10

[a]ASP means aspirin; COL means cholesterol; NAP means naproxen; IBU means ibuprofen; ACPH means acetaminophen. [b]C_I is the concentration of solute in the initial organic solution, [c]CO_2 content, X_W = CO_2 molar fraction in the solvent mixture. [d]Temperature decrease, $\Delta T = T_F - T_W$. [e]Absolute supersaturation, $\Delta C = C_I - C_F^S$. [f]Supersaturation ratio $S = C_I/C_F^S$. [g]Crystallization yield = 100·(recovered mass of solids/initial mass of solids). [h]Volumetric particle size distributions are described by $d(0.1)$, $d(0.5)$, and $d(0.9)$, which are the particles diameters (μm) under which there are 10%, 50%, and 90% of the total volume of the particles, respectively. $d(0.5)$ is the volume median particle diameter. [i]Uniformity index is defined as UI = $d(0.1)/d(0.9) \times 100$.

when the CO_2 content is increased from 0.50 to 0.64. As discussed in section 3.1, this result can be explained by the larger temperature reduction achieved during the depressurization step (ΔT): augmenting this temperature reduction ΔT provokes a decrease in C_S^F, and a more pronounced increase of the supersaturation attained during the depressurization of the

dx.doi.org/10.1021/cg200356x | Cryst. Growth Des. 2012, 12, 1717–1726

CO_2-expanded solution (Step 3 in Figure 1), that favors nucleation over crystal growth, therefore obtaining smaller particle sizes.

To test the effect of the initial solute concentration (C_I), experiments ASP3-ASP4 and COL3-COL4 were performed varying C_I while keeping constant the rest of the operating parameters. As expected, for each solute, at constant P_W, T_W, and CO_2 content, particle size decreases with increasing C_I. In aspirin experiments ASP3-ASP4, increasing C_I from 3.5×10^{-2} mol/mol to 5.2×10^{-2} mol/mol results in a medium particle size reduction from 30.5 to 16.5 μm, due to an increase of the supersaturation ratio S from 1.3 to 1.9. Cholesterol crystallizations COL3-COL4 showed a particle reduction from 2.1 to 1.2 μm when C_I was increased from 2.6×10^{-3} mol/mol to 3.8×10^{-3} mol/mol, which caused S to rise from 9 to 13.

In summary, the higher the X_W and C_I values, the higher the supersaturation attained in the experiment, which contributes to a decrease the size of the crystals produced. Nevertheless, X_W and C_I cannot be increased without limit, since the drug solubility behavior in the CO_2- expanded solvent limits the operating conditions (see Figure 2).

Experiments ASP2-ASP3 (Figure 2) and COL2-COL3, performed along the solubility curve, were used to compare the weight of C_I and X_W parameters on the supersaturation achieved and on particle characteristics, and discern which parameter yields a more important decrease in particle size. Results in Table 2 show that experiment ASP3, performed at lower C_I and higher X_W ($C_I = 5.2 \times 10^{-2}$ mol/mol, $X_W = 0.55$) than ASP2 ($C_I = 7.0 \times 10^{-2}$ mol/mol, $X_W = 0.47$), presents a larger particle size reduction ($d(0.5)_{ASP3} = 16.5$ μm, $d(0.5)_{ASP2} = 23.4$ μm). In contrast, COL2 experiment, performed at higher C_I and lower X_W ($C_I = 5.1 \times 10^{-3}$ mol/mol, $X_W = 0.64$) than COL3 ($C_I = 3.8 \times 10^{-3}$ mol/mol, $X_W = 0.71$), yields the smallest particles ($d(0.5)_{COL2} = 0.5$ μm, $d(0.5)_{COL3} = 1.2$ μm). The reason for the observed different weights of C_I and X_W on particle characteristics of aspirin and cholesterol experiments can be rationalized as follows, taking into account the supersaturation evolution which occurred during the three steps of the process studied, represented in Figure 1.

Absolute supersaturation values ΔC for experiments ASP2-ASP3 and COL2-COL3, also shown in Table 2, have been represented in Figure 5, using the solubility evolution of aspirin and cholesterol with temperature, also represented in the same figure as curves fitted to experimental solubility measurements. As Figure 5 shows, in the temperature range studied aspirin solubility in acetone decreases linearly with decreasing temperature. Therefore, in aspirin crystallizations, achieving a lower depressurization temperature results in a remarkably lower solubility at T_F. When comparing supersaturation values of experiments ASP2-ASP3, it can be observed that ΔC^{ASP3} (0.024 mol/mol) is slightly higher than ΔC^{ASP2} (0.022 mol/mol), since the difference between solubility at the final temperature, C_F^S, of ASP3 and ASP2 is higher than the difference between the initial concentrations C_I of both experiments. This observation explains the higher particle size reduction obtained in ASP3. In contrast, Figure 5 shows that for cholesterol experiments, ΔC^{COL2} (0.0048 mol/mol) is remarkably higher than ΔC^{COL3} (0.0035 mol/mol). The solubility variation of cholesterol in acetone shows an exponential behavior, with no significant variation of solubility at temperatures below 275 K. As discussed before, increasing the CO_2 content X_W results in a decrease in the

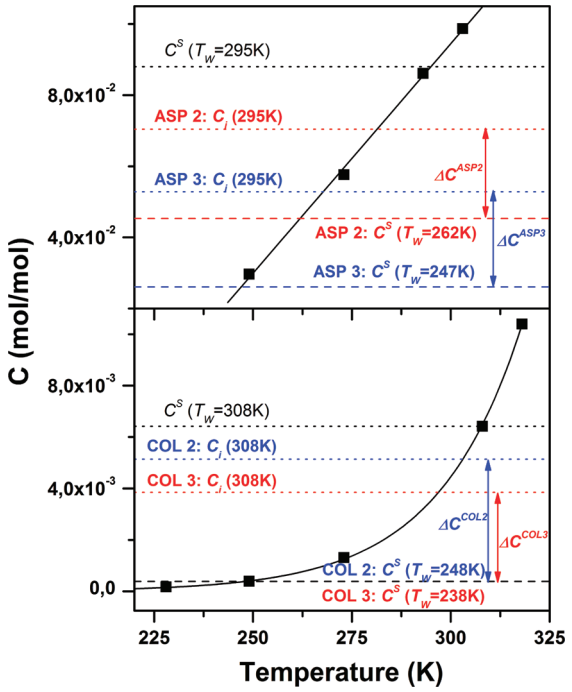

Figure 5. Solubility versus temperature evolution of (top) aspirin and (bottom) cholesterol in acetone solutions. Experimental measurements (■) obtained through a static gravimetric method were fitted to linear and exponential functions for aspirin and cholesterol, respectively. Degrees of absolute supersaturation $\Delta C = C_I - C_F^S$ obtained in each experiment are also represented.

depressurization temperature T_F. In this case, increasing the CO_2 content of the mixture to reach a lower T_F will not result in a significant increase of the supersaturation attained, and the variation of the initial concentration C_I will produce a more pronounced effect on the supersaturation achieved in the crystallization. In experiments COL2-COL3, the difference in supersaturation is governed by the difference in the initial concentration.

Therefore, in ASP3 and COL2 it has been possible to reach higher supersaturation values, and consequently higher nucleation rates, than in ASP2 and COL3, respectively, allowing the formation of smaller particle sizes. Summarizing, in aspirin experiments performed over the solubility curve, an increase in X_W is more dominant producing higher supersaturations than an increase in C_I. Conversely, in cholesterol experiments higher C_I values are revealed as more important than higher X_W values, since cholesterol solubility (C_F^S) does not change significantly from 275 K to lower temperatures, whereas the solubility of aspirin changes linearly with temperature. Therefore, it is possible to predict the relative weight of process parameters C_I and X_W on particle characteristics by simply determining the solubility variation with temperature of the compound to be crystallized in the corresponding organic solvent at atmospheric pressure.

It should also be pointed out that yields obtained in cholesterol crystallizations are remarkably higher than those obtained in aspirin crystallizations from acetone/CO_2. Experiment COL2 produced a yield of 85% in mass of particles produced, whereas ASP3 produced a 40% yield. The reason for the difference in effectiveness of the crystallization process studied is again a consequence of the different solubility rise with temperature seen in Figure 5. In cholesterol experiments,

dx.doi.org/10.1021/cg200356x | Cryst. Growth Des. 2012, 12, 1717–1726

Table 3. Scale-Up Experiments Performed from "Acetone/CO_2" Mixtures with Aspirin As a Model Drug

									diameter of particles[a] (μm)		
exp	vessel vol (mL)	expanded mixture	P_W (MPa)	T_W (K)	C_I (mol/mol)	X_W	yield (%)	ΔT (K)	$d(0.1)$	$d(0.5)$	$d(0.9)$
ASP3	300	acetone/CO_2	7	295	5.2×10^{-2}	0.55	40	−48	5.9	16.5	42.6
ASP6	2000	acetone/CO_2	7	295	5.2×10^{-2}	0.55	40	−45	4.7	15.0	41.0

[a]Volumetric particle size distributions are described by $d(0.1)$, $d(0.5)$, and $d(0.9)$, which are the particles diameters (μm) under which there are 10%, 50%, and 90% of the total volume of the particles, respectively. $d(0.5)$ is the volume median particle diameter.

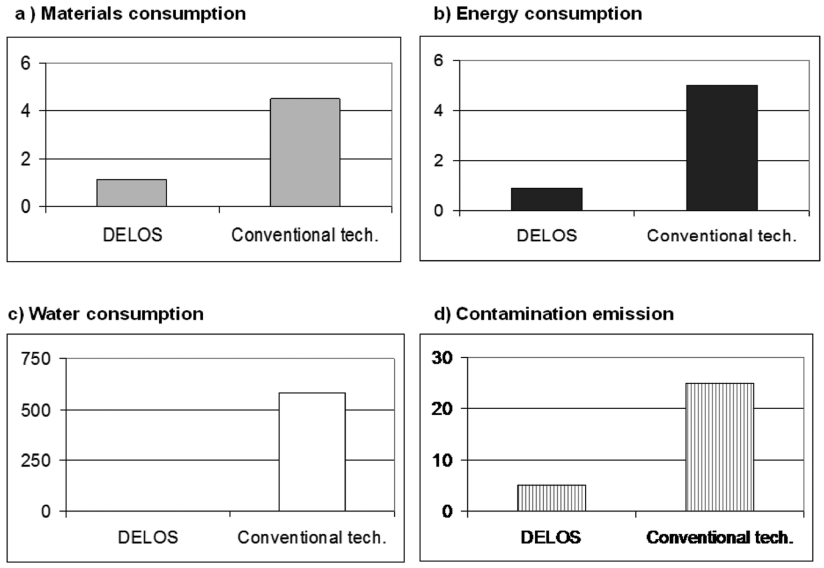

Figure 6. Calculated sustainability indexes of a theoretical industrial GMP multiproduct plant for producing 50 tonnes per year of micrometer-sized API, versus real indexes of a real conventional crystallization pharmaceutical plant of the same capacity.[13] (a) Materials Index: kg of consumed raw materials per kg of final product. (b) Energy index: kg of consumed natural gas (kg of gas equivalents to kJ of gas, oil, electricity, and steam) per kg of final product. (c) Water index: kg of consumed water (process and utility water) per kg of final product. This plant design does not consume water. (d) Contamination index: kg of greenhouse gases emitted per kg of final product.

solubility at T_F is an order of magnitude lower than solubility at T_W (10^{-4} mol/mol vs 10^{-3} mol/mol). This fact allows the production of a very powerful supersaturation increase during the depressurization step provoking the crystallization of most of the compound dissolved before this step. On the other hand, in aspirin experiments from expanded acetone, when temperature decreases from T_W to T_F, the solubility of the compound is only lowered to a half. Hence, the supersaturation generated is less important than in the case of cholesterol and consequently an important mass of aspirin remains in solution despite the temperature decrease. However, as Table 2 shows, experiment ASP5 performed using expanded ethanol gave an 80% yield of powdered aspirin, compared with 40% obtained in ASP4 from expanded acetone. Crystallization yield of processed aspirin can be remarkably improved by using CO_2 expanded ethanol as the medium, since solubility variation with temperature of aspirin in ethanol is higher than that in acetone.

4. INDUSTRIAL VIABILITY OF THE DELOS PROCESS

The process studied was successfully scaled-up by 7-fold from laboratory (300 mL vessel volume) to pilot plant scale (2000 mL) by performing precipitation experiments using aspirin as a model drug. Experiments at each scale were repeated twice with reproducible results. The results, summarized in Table 3, show an extremely high reproducibility, both in terms of particle size and precipitation yield. The scale-up design was simply done by geometric factors, since the technical complexity of the required equipment is very low. Compared with conventional crystallizations from liquid solvents, the inherent features of the crystallization process studied make it very easy to scale-up, avoiding classical scaling-up troubles such as those related to agitation. In conventional cooling crystallizations, the stirring rate and the stirrer design determine the supersaturation homogeneity and therefore the homogeneity in particle size. When scaling up, this parameter becomes critical: the bigger the crystallization vessel, the bigger the gradient temperature from the vessel walls to the center, giving very heterogeneous supersaturation profiles and poor reproducibility which complicate scale-up thereof. Since in the process studied the stirring is only used in the pressurization step, to achieve a faster mixing of the CO_2 with the organic solvent, and it is not needed in the depressurization step, where the crystallization occurs, the homogeneity of the supersaturation achieved is independent of the vessel volume and the stirring rate is not affecting the final characteristics of the precipitated particles. Another remarkable point which eases a scale-up design of the reported crystallization method is the fact that the depressurization takes place by just opening a simple valve.

Even so, the industrial application of this process will only be possible if, at the present process development stage, it can be shown to be industrially viable from the technical, economical, and environmental points of view. For this purpose, in a recent study, we have evaluated the feasibility of this crystallization method for the industrial production of micrometer or submicrometer-sized particulate drugs.[13] On the basis of experimental data, we first designed a cGMP (Good

dx.doi.org/10.1021/cg200356x | Cryst. Growth Des. 2012, 12, 1717−1726

Manufacturing Practices) multiproduct plant for producing 50 tonnes of micrometer-sized APIs per year. The design turned out to be perfectly viable according to GMP's rules, since the following characteristics, among others, are easily achieved: process parameters are easily registered; closed equipment is used, avoiding exposure of the workers to the products and exposure of the products to the atmosphere, and the entire process is performed in a single area, avoiding transport and loss of material from unit to unit and decreasing product contamination risks. Compared with conventional multistep procedures, decreasing process units also simplifies the related quality documentation. The high reproducibility and batch-to-batch consistency of the process studied also allow the recirculation of the mother liquor in the subsequent crystallization cycle, which has been limited to a given number of recirculations. Finally, the cleaning of the equipment after each batch can be done by using CO_2-expanded solvents at high pressure, and its efficiency evaluated by analyzing samples of the cleaning solvent.

From the technical point of view, the equipment needed for building an industrial plant is already available. During recent years, industrial supercritical CO_2 extraction facilities, which use similar pressure vessels and related equipment, and which work at higher working pressures and use bigger vessel volumes than the ones required for a plant working under the methodology described, have been produced around the world.[26] Hence, technically, an industrial scale-up is perfectly viable.

The evaluation of the environmental sustainability of this process, compared with conventional crystallizations from liquid solvents, also showed very interesting results. Figure 6 represents the sustainability indexes of the designed plant versus a real conventional crystallization pharmaceutical plant of the same capacity. Sustainability indexes are quantitative indicators that account for the necessary amount of materials, energy, water needed, and contamination emitted for producing 1 kg of product.[27] The materials index represents the kilogram of consumed raw materials per kilogram of final product, the energy index accounts for the kilogram of consumed natural gas (kilogram of gas equivalents to kJ of gas, oil, electricity, and steam) per kilogram of final product, the water index represents the kilogram of water consumed (process and utility water) per kilogram of final product, and the contamination index shows the kilogram of greenhouse gases emitted per kilogram of final product. Sustainability indexes have been calculated from mass and energy balances. In all cases, the indexes of the designed plant were significantly lower than the corresponding to the conventional crystallization plant, meaning that the studied crystallization process is a greener and environmentally more friendly process than conventional pharmaceutical crystallization procedures.

Preliminary economic aspects were also estimated. The total capital investment required for the CF-based plant, estimated from equipment costs, according to the multiplying factors method reported by Peter, Timmerhaus and West,[28] turns out to be much lower (~10 times lower) than the investment required for a real pharmaceutical crystallization plant of the same capacity.[13] Thus, the comparison of environmental and economic aspects of the designed plant with real conventional multistep crystallization processes, reveals important and attractive advantages of the CO_2-based process.

5. CONCLUSIONS

The DELOS process, based on the use of compressed fluids, is an efficient crystallization method for the one -step production of crystalline micrometer-sized particles of active pharmaceutical ingredients, such as aspirin, cholesterol, naproxen, ibuprofen, and acetaminophen, with high polymorphic purities and no detectable residual solvent content by TGA. In addition, the actual particle size of the processed powders can be modulated by controlling operational parameters, such as the CO_2 content of the expanded solution, and the concentration of the initial solution. The influence of these process parameters on nucleation rates and on products characteristics can be predicted from solubility data through the methodology presented here for the first time. This new process can provide real advantages over conventional crystallization processes, such as (1) high purity products, (2) control of crystal polymorphism, (3) in-process elimination of residual solvent/reduction of residual solvent levels, (4) processing of thermolabile and waxy compounds, (5) single-step in single-area process, (6) easy and reproducible scale-up, (7) environmentally friendly technology, (8) technically and economically viable process at industrial scale.

However, the slow implementation rates of compressed fluids-based methodologies at industrial level could be attributed to the strict and inflexible requirements that pharmaceutical companies have to satisfy for changing their production procedures.

AUTHOR INFORMATION

Corresponding Author

*E-mail: ventosa@icmab.es (N.V.), vecianaj@icmab.es (J.V.).

ACKNOWLEDGMENTS

This work was supported by grants from DGI, Spain, projects CONSOLIDER-C EMOCIONA (CTQ2006- 06333/BQU), POMAS (CTQ2010- 019501), and NANOFAR (NAN2004-09159-C04-01) and to DGR, Catalunya (project 2005SGR 00591). We acknowledge financial support from Instituto de Salud Carlos III, through "Acciones CIBER". The Networking Research Center on Bioengineering, Biomaterials and Nanomedicine (CIBER-BBN) is an initiative funded by the VI National R Plan 2008-2011, Iniciativa Ingenio 2010, Consolider Program, CIBER Actions and financed by the Instituto de Salud Carlos III with assistance from the European Regional Development Fund. E. Moreno acknowledges the MICINN for a Juan de la Cierva postdoctoral contract. E. Rojas thanks the CSIC for her PhD bursary. Nora Ventosa thanks Banco de Santander for the chair of Knowledge and Technology Transfer Parc de Recerca UABSantander. We also thank TECNIO network for financial support on technological transfer activities related to this work. We also thank R. Solanas (ICMAB) for the operation of high-pressure facilities at the ICMAB, Dr. Ricard Alvarez and Dr. Jaume Comas for their assistance during the performance of particle size measurements, as well as the UAB Microscopy service for their help in recording SEM images. We would like to thank Prof. Gurnos Jones for the English revision and correction of the manuscript.

REFERENCES

(1) (a) Jinno, J.; Kamada, N.; Miyake, M.; Yamada, K.; Mukai, T.; Odomi, M.; Toguchi, H.; Liversidge, G.; Higaki, K.; Kimura, T. *J.*

Controlled Release **2006**, *111*, 54−64. (b) Yu Shekunov, B.; York, P. *J. Cryst. Growth* **2000**, *211*, 122.
(2) Otsuka, M.; Kaneniwa, N. *Int. J. Pharm.* **1990**, *62* (1), 65.
(3) Banakar., U. V., Ed. Pharmaceutical Dissolution Testing. In *Drugs and the Pharmacutical Sciences Series*; Marcel Dekker: New York, 1992; Vol. *49*.
(4) (a) Findlay, G. F. *Kermani; Novel Drug Delivery Technologies and Drug Development Business Briefing - PharmaTech* **2001**, 166. (b) Samler, C. *Eur. Pharm. Rev.* **1998**, *4*, 61−63. (c) Bennet, J.; Nichols, F.; et al. *J. Oral Maxillofacial Surg.* **1998**, *56* (11), 1249−1254. (d) Obeye, J.; Mannaerts, B.; et al. *Hum. Reprod.* **2000**, *15* (2), 245−249.
(5) International Conference for Harmonisation of Technical Requirements for Registration of Pharmaceuticals for Human Use. ICH. Harmonised Tripartite Guideline Impurities: Guideline for Residual Solvents Q3C(R4). Current Step 4 version dated February 2009. Parent Guideline dated 17 July 1997.
(6) (a) Jung, J.; Perrut, M. *J. Supercrit. Fluids* **2001**, *20*, 179. (b) Wei, M.; Musie, G. T.; Busch, D. H.; Subramaniam, B. *J. Am. Chem. Soc.* **2002**, *124*, 2513.
(7) Palakodaty, S.; York., P. *Pharm. Res.* **1999**, *16*, 976.
(8) Foster, N.; Mammucari, R.; Dehghani, F.; Barret, A.; Bezanehtak, K.; Coen, E.; Combes, G.; Meure, L.; Regtop, A.; Tandya, A. *Ind. Eng. Chem. Res.* **2003**, *42*, 6479.
(9) Ventosa, N.; Sala, S.; Torres, J.; Llibre, J.; Veciana, J. *Cryst. Growth Des.* **2001**, *1*, 299.
(10) Ventosa, N.; Veciana, J.; Rovira, C.; Sala, S. (Carburos Metàlicos S.E.). Method for Precipitating Finely Divided Solid Particles PCT/ES01/00327, August 2000.
(11) Ventosa, N.; Sala, S.; Veciana, J. *J. Supercrit. Fluids* **2003**, *26*, 33.
(12) Mullin, J. W. *Crystallization*; Butterworth Heinemann, Oxford, 2000; p 189.
(13) A. Córdoba. Disseny d'una planta DELOS per a l'obtenció de materials moleculars microparticulats d'interès farmacèutic. Master Thesis, Chemical Engineering Department, Universitat Politècnica de Catalunya. 2009.
(14) Wubbolts, F. E. Ph.D. Thesis: Supercritical crystallization. Volatile components as (anti-) solvents. Universal Press Science Publishers: The Netherlands, 2000; p 50.
(15) Gimeno, M.; Ventosa, N.; Veciana, J.; Boumghar, Y.; Fournier, J.; Boucher, I. *Cryst. Growth Des.* **2006**, *6*, 23−25.
(16) Cano-Sarabia, M.; Ventosa, N.; Sala, S.; Patiño, C.; Arranz, R.; Veciana, J. *Langmuir* **2008**, *24*, 2433−2436.
(17) Muntó, M.; Ventosa, N.; Sala, S.; Veciana, J. *J. Supercrit. Fluids* **2008**, *47*, 147−153.
(18) Sala, S.; Tassaing, T.; Ventosa, N.; Danten, Y.; Besnard, M.; Veciana, J. *ChemPhysChem* **2004**, *5*, 243.
(19) Sala, S.; Elizondo, E.; Moreno, E.; Calvet, T.; Cuevas-Diarte, M. A.; Ventosa, N.; Veciana, J. *Cryst. Growth Des.* **2010**, *10*, 1226−1232.
(20) Wheatley, P. J. *J. Chem Soc.* **1964**, 6036.
(21) Vishweshwar, P.; McMahon, J. A.; Oliveira, M.; Peterson, M. L.; Zawarotko, M. J. *J. Am. Chem. Soc.* **2005**, *127*, 16802.
(22) Shieh, H. S.; Hoard, L. G.; Nordman, C. E. *Acta Crystallogr.* **1981**, *B37*, 1538.
(23) Haisa, M.; Kashino, S.; Kawai, R.; Maeda, H. *Acta Crystallogr.* **1976**, *B32*, 1283.
(24) Kim, Y. B.; Song, J.; Park., I. Y. *Arch. Pharm. Res.* **1987**, *10*, 232.
(25) McConnell, J. F. *Cryst. Struct. Commun.* **1974**, *3*, 73.
(26) Perrut, M. *Ind. Eng. Chem. Res.* **2000**, *39*, 4531−4535.
(27) Bonanza, N. Estudi de sostenibilitat comparatiu dels processos batch vs continu en la hidrogenació d'olis. Master Thesis, Chemical Engineering Department, Universitat Politècnica de Catalunya, 2005.
(28) West, M. S.; Timmerhaus, K.; West, R. E., Eds.; *Plant Design and Economics for Chemical Engineers*, 5th ed.; McGraw-Hill: New York, 2003.